Original Research Article: full paper

(2023), «EUREKA: Physics and Engineering» Number 4

EFFECT OF LOADING PATHS ON HYDROFORMING ABILITY OF STEPPED HOLLOW SHAFT COMPONENTS FROM DOUBLE LAYER PIPES

Quang Duc Vu✉
Department of Metal Forming[1]
Department of Machines & Fundamentals of Machine Design[2]
vuquang@uneti.edu.vn

Trung Dac Nguyen
Department of Metal Forming[1]

Hoa Van Dang
Department of Machinery Manufacturing Technology[2]

Duc Trong Phan
Department of Mechatronics[2]

[1]*Hanoi University of Science and Technology*
1 Dai Co Viet, Bach Khoa ward, Hai Ba Trung district, Hanoi, Vietnam, 100000

[2]*University of Economics – Technology for Industries*
456 Minh Khai, Vinh Tuy Ward, Hai Ba Trung District, Hanoi, Vietnam, 100000

✉**Corresponding author**

Abstract

The step hollow shaft components are composed of two layers of different materials, they are formed using tube hydroforming process due to its high strength and rigidity, low weight and flexible profiles, compared to traditional casting, welding, and forming methods. These products are effectively used in industries such as the automotive, shipbuilding, aerospace and defense, and oil and gas sectors. The success of various double layer pipe hydroforming process depends on several factors, with the most important being the internal pressure path and axial loading path. This paper presents research on the effect of input loading paths on the hydroforming ability of a different two-layer metal structure – an outer layer of SUS304 stainless steel and an inner layer of CDA110 copper – using 3D numerical simulations on Abaqus/CAE software. Output criteria were used to evaluate the forming ability of the formed components, including Von Mises stress, Plastic strain component (PEmax), wall thinning, and pipe profile, based on which the input loading paths were combined during the forming process. These output criteria allow for more accurate predictions of material behavior during the hydroforming process, as well as deformation and stress distribution. This can support the design process, improve product quality, reduce errors, and increase production efficiency. The research results can be applied as a basis for optimizing load paths for the next experimental step in the near future, for undergraduate and graduate training, as well as allowing designers and engineers to optimize the process of hydroforming of different 2-layer tubes, reducing costs, improving accuracy, flexible design, minimizing risks, and increasing efficiency.

Keywords: different double layer pipes, loading paths, tube hydroforming, 3D numerical simulations.

DOI: 10.21303/2461-4262.2023.002797

1. Introduction

Tube hydroforming is a highly sought-after alternative to traditional forming methods, becoming increasingly prevalent [1, 2]. The outcomes of this forming process are utilized across numerous industries, such as automotive, aerospace, shipbuilding, and oil and gas [3–6]. Additionally, microtubes for electrical and electronic components can also be produced using this process [7–9]. The strengths and weaknesses of this technique, as well as its growth and application, have been thoroughly discussed in numerous resources [10, 11].

Utilizing the finite element method and advanced 3D numerical simulations in the design of tube hydroforming processes has been demonstrated to be efficient in evaluating input and output parameters, resulting in cost and time savings [12, 13]. Several advanced numerical model-based approaches

have been introduced and implemented by various researchers [14–16]. Additionally, simple methods have also been offered to assist in the preliminary design of metal forming processes, such as the ideal flow theory in plastic deformation [17] and sheet forming with optimal deformation [18]. A concise solution, based on integral equations, has been presented to examine the relationship between parameters during 2-layer tube shaping [19]. Simple solutions for determining the maximum value of P_i are critical for estimating the required forming pressure during water tube forming of coated tubes [20]. Modeling has also been utilized to simulate the transverse branch swelling of coated bimetallic tubes [21].

The utilization of hydrostatic shaped multi-layer pipe products has increased because of their remarkable properties. These laminated tubes, which possess combined material properties, high strength, and corrosion resistance, are used in specialized work environments to meet conflicting performance requirements. In order to predict the most efficient operating conditions, a finite element model was developed for the two-layer tubular forming process using the LS-DYNA preprocessor and ANSYS LS-DYNA solver. The model was validated through experiments, which showed that the numerical and experimental results for the bulge height and thickness reduction of the 2-layer X-shaped tube agreed well [22]. An analytical model has also been developed to estimate the forming pressure required to avoid creasing in double-layer pipe joints [23]. By comparing experimental and numerical simulation results, it was found that the most significant cause of pipe breakage is due to the internal pressure applied to the part without proper axial feed application and failure to follow the load curve [24].

During tube hydroforming process, three types of errors may occur: burst, wrinkles, and excessive thinning. Optimal loading conditions must be established to avoid these instability and failure conditions and ensure proper deformation. Due to the complexity of the process, analysis and numerical simulation are necessary to better understand it and design process equipment.

The authors utilized finite element numerical simulation with Abaqus/Explicit 3D EXPERIENCE R2017X software [25] on the basis of Materials and Methods presented in detail in the next Section 2 to assess the forming capability of stepped hollow shaft components from 2 different material layers using hydroforming techniques. The simulations investigated the outcome of combining the internal pressure load line and the axial feed load line, thereby determining the optimal loading lines for the different two-layer tube hydroforming process. From the research results, the team proposed optimal load lines for successful hydroforming process according to 4 output criteria including Von Mises stress, Plastic strain component (PE_{max}), wall thinning, and pipe profiles of double-layer pipes of different materials are formed into step hollow shafts with an outer layer of SUS304 material and an inner layer of CDA110 material.

2. Materials and Methods

2. 1. Hydroforming component and original workpiece

This study utilized a setup with an initial tube billet, which has 2 different material layers for numerical simulation, with stainless steel SUS304 selected as the outer layer and copper CDA110 as the inner layer. The material properties of the workpiece are detailed in **Table 1**, while **Table 2** presents the billet parameters and composition of the step hollow shaft.

Table 1

Material properties of SUS304 and CDA110 [10, 11]

Material properties	SUS304/Value	CDA110/Value
Temperature (°C)	24	24
Density, ρ (kg/m^3)	7850	8940
Young's modulus, E (GPa)	193	115
Hardening coefficient, K (MPa)	1275	325
Work hardening exponent, n	0.45	0.54
Poisson's ratio, ν	0.29	0.33
Yield strength (MPa)	226.3	170
Ultimate tensile strength (MPa)	560	425
Elongation (%)	45	45

Table 2

Double layer pipe blank and step hollow shaft component parameters

Parameters	Symbol/unit	Value
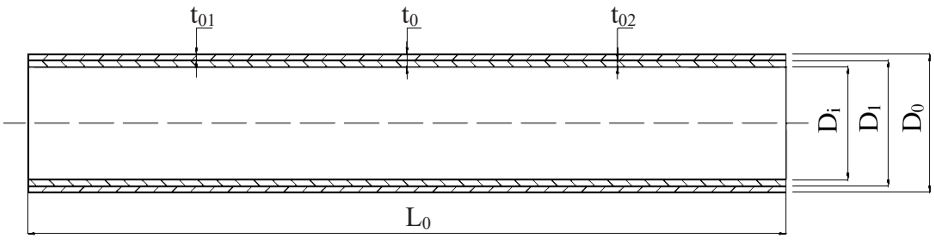		
Outer diameter of double-layer pipe billet	D_0 (mm)	21.80
Diameter of separator between 2 layers of material SUS304 and CDA110	D_1 (mm)	19.30
Inside diameter of double-layer pipe billet	D_i (mm)	18.10
Initial thickness of material layer SUS304	t_{01} (mm)	1.25
Initial thickness of material layer CDA110	t_{02} (mm)	0.6
Initial thickness of double-layer pipe billet	t_0 (mm)	1.25+0.6 = 1.85
Initial length of double-layer pipe billet	L_0 (mm)	120
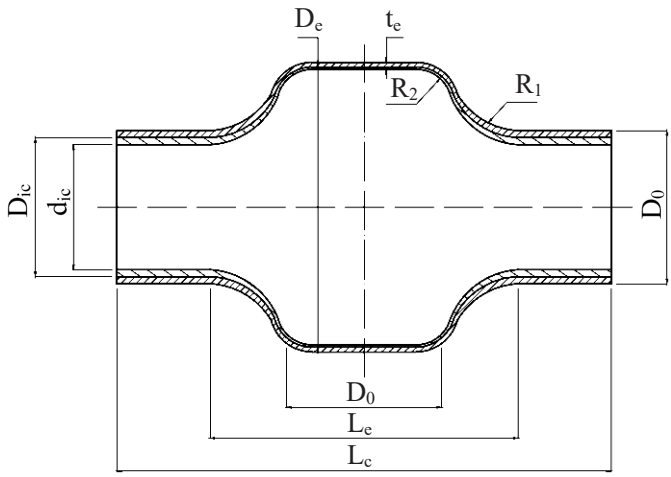		
Maximum expanded diameter	$D_e = 1.8D_0$ (mm)	39.24
Diameter of separator between 2 layers of pipe component	D_{ic}	to be formed
Inside diameter of pipe component	d_{ic}	to be formed
Thickness of component	t_c (mm)	to be formed
Transition fillet radius	R_1 (mm)	20
Expansion fillet radius	R_2 (mm)	10
Unsupported length of tool for maximum expansion	L_e (mm)	43.6
Length of double-layer pipe component	L_c (mm)	to be designed

2. 2. Numerical simulation

The hydrostatic forming of 2-layer metal pipes can be modeled through numerical simulation, utilizing finite element analysis and finite element method. This enables researchers to visualize the shaping process and evaluate the forming parameters. To simulate the process, a cylindrical double-layer tube with a total thickness of 1.85 mm, outside diameter of 21.80 mm, and length of 120 mm is inflated into a step hollow shaft with a maximum extension diameter of 39.24 mm, calculated as 1.8 times the outside diameter. The tube is initially modeled as two separate blocks, with the outer layer made of SUS304 and 1.25 mm thick, and the inner layer made of CDA110 and 0.6 mm thick, both of which use a bi-linear elastic material model as shown in **Table 1**. The coefficient of friction between the surfaces of the SUS304 and CDA110 materials is assumed to be zero,

while the coefficient of friction between the remaining surfaces of the workpiece and the tool is set to 0.1 [26]. Using symmetry and precise boundary conditions, a one-eighth segment of the problem can be modeled, resulting in a suiTable three-dimensional solution. The bulge forming process is simulated using the finite element model in **Fig. 1**.

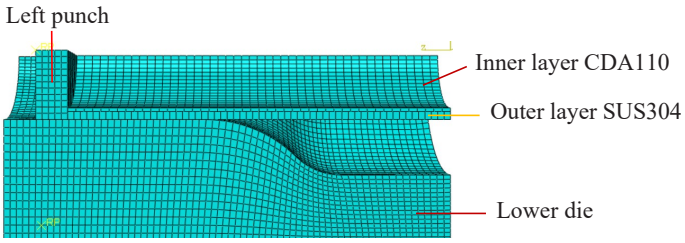

Fig. 1. Assembly and mesh modules used in the bimetallic tube analysis

The same finite element model was used to perform simulations with combined internal pressure load paths (**Fig. 2**) and axial feed load paths (**Fig. 3**).

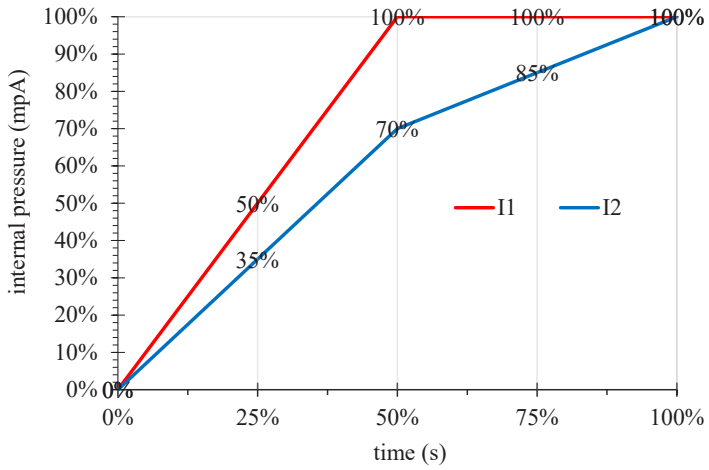

Fig. 2. Internal pressure load lines

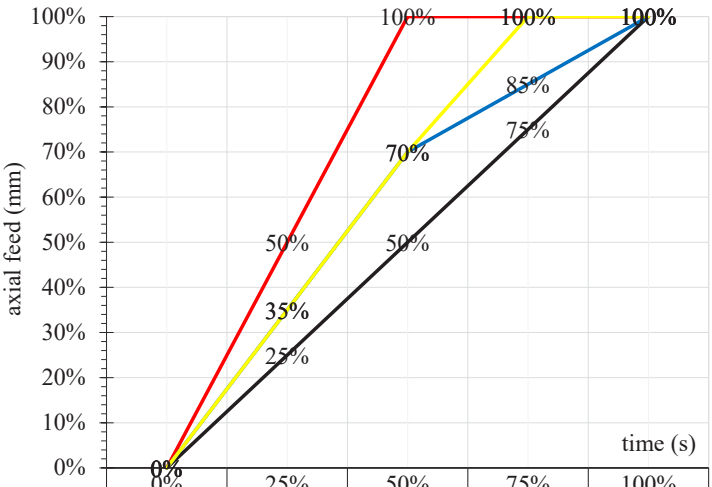

	0%	25%	50%	75%	100%
A1	0	0.5	1	1	1
A2	0	0.25	0.5	0.75	1
A3	0	0.35	0.7	0.85	1
A4	0	0.35	0.7	1	1

Fig. 3. Axial feed load lines

3. Results and Discussion

3. 1. Combined internal pressure load line I1 and axial feed load line A2

Three simulations were conducted, combining the internal pressure load line *I*1 with $P_{i\text{-max}}$ values of 45, 55, 65 MPa, and the axial feed line *A*2, where each punch has a displacement of 10 mm, resulting in a total axial feed of 20 mm. The simulations were named P45I1-Af10A2, P55I1-Af10A2, and P65I1-Af10A2, corresponding to maximum internal pressure values of 45, 55, and 65 MPa. The forming results of simulations 1, 2, and 3 are presented in **Fig. 4** in the order of **Fig. 4, *a***, ***b***, and **Fig. 4, *c*, *d***.

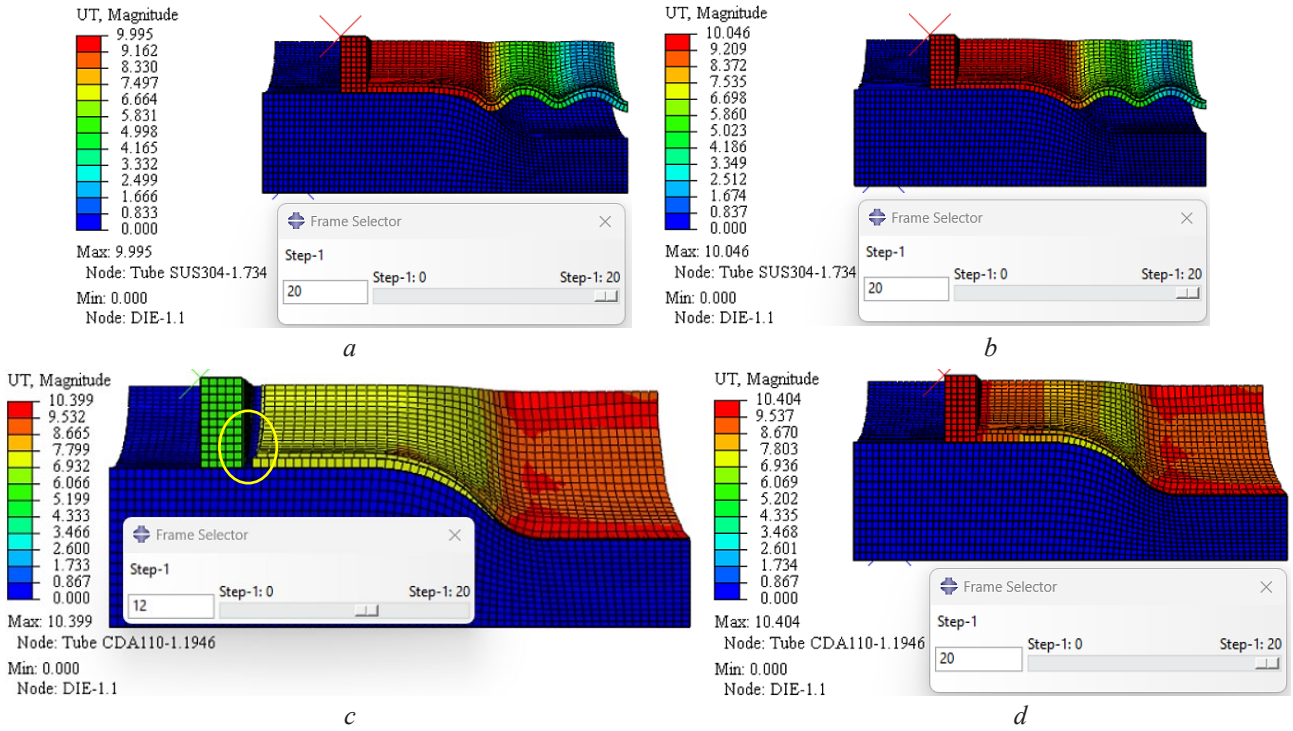

Fig. 4. Shaped bilayer components:
a – P45I1 – Af10A2; *b* – P55I1 – Af10A2; *c* and *d* – P65I1 – Af10A2

Simulations 1 and 2 yielded unsatisfactory component profiles, with wrinkled-corrugated expansion zones, and the material did not fully expand into the entire mold cavity. In these simulations, axial feeding was fast, and the sealing requirement was guaranteed within 20 steps with $P_{1\text{-max}}$ at 45 MPa and $P_{2\text{-max}}$ at 55 MPa. On the other hand, simulation 3 showed that the axial feeding was slow, resulting in the sealing requirements not being guaranteed within steps 12–14, and failing to meet the requirement for timely feeding of the workpiece in the expansion area. Consequently, both layers of material experienced strong plastic deformation, with a plastic deformation component $PE_{3\text{-max}}$ (CDA110) of 1.755, and significant thinning with a minimum material thickness of 0.07 mm/0.6 mm (thinning ratio of 83.33 %). Similarly, $PE_{3\text{-max}}$ (SUS304) was strongly thinned with a minimum material thickness of 0.16 mm/1.25 mm (thinning ratio of 87.20 %).

Based on the data analysis of the simulation, it can be concluded that the plan to combine the load lines during the forming process did not meet the evaluation criteria for forming components. To enhance the forming ability, it is suggested to increase the total axial feed and the internal pressure.

3. 2. Combined internal pressure line I1 and axial load line A1/A3

Based on the results and analysis above, the research team made adjustments to the axial billet feeder, increasing it to 30 mm total, and modified the axial feed load line to *I*1 and *I*2 load lines. The internal pressure load line is still the load line *I*1 with $P_{i\text{-max}}$ values of 60 and 75 MPa. These modi-

fications were used in three simulation runs where the internal pressure load line and the axial feed load line were combined together. The simulations were run with $P_{4\text{-max}} = 60$ MPa (P65I1-Af15A1), $P_{5\text{-max}} = 75$ MPa (P75I1-Af15A1), and $P_{6\text{-max}} = 75$ MPa (P65I1-Af15A3). The results of these simulations 4, 5, and 6, are presented in **Fig. 5** in the order of **Fig. 5, *a*–c**.

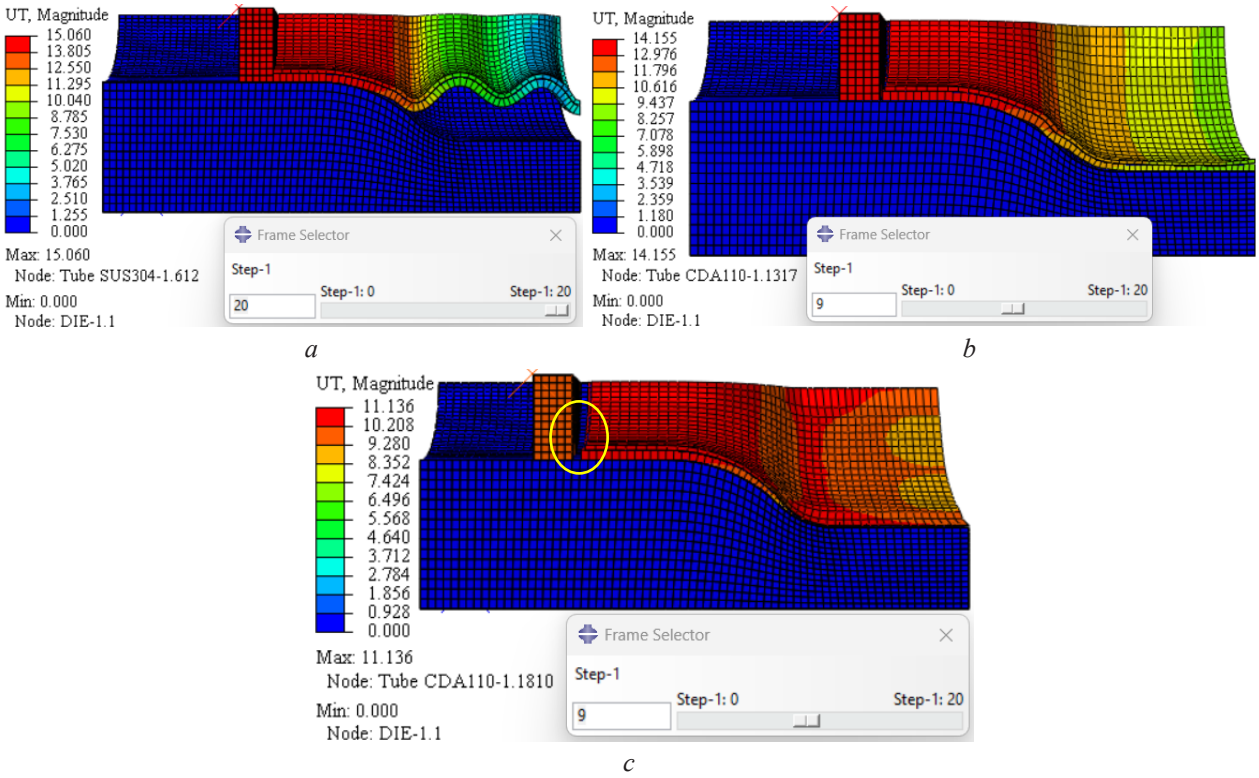

Fig. 5. Shaped bilayer components: *a* – P65I1 – Af15A1; *b* – P75I1 – Af15A1; *c* – P65I1 – Af15A3

The findings of simulation 4 reveal an incomplete component profile, characterized by an expansion zone with a wrinkled-corrugated profile, indicating that the material has not expanded to fill the entire mold cavity. The simulation demonstrates that the axial feed is quite fast, ensuring that the sealing requirement is guaranteed in 20 steps. However, the internal pressure $P_{4\text{-max}} = 60$ MPa is still small to achieve satisfactory results.

The results of simulation 5 indicate a slow axial feed, resulting in the sealing requirement not being met at step 9 and the workpiece not being fed in the extended area in a timely manner. Both layers of the material experienced plastic deformation, with the plastic deformation component $PE_{5\text{-max}}$ (CDA110) = 0.81, and significant thinning occurred, with the smallest material thickness reaching 0.32 mm/0.6 mm (a thinning ratio of 46.47 %); similarly, $PE_{5\text{-max}}$ (SUS304) = 0.72 with a minimum material thickness of 0.76 mm/1.25 mm (a thinning ratio of 39.20 %). Although component profiles are well-formed, delamination occurs in the transition zone between radii R_1 and R_2.

Simulation 6 resulted in slow axial feed, leading to failure to guarantee sealing requirements at steps 9 and 10 and timely feeding of the workpiece into the extended area. Consequently, both layers experienced plastic deformation with the plastic deformation component $PE_{6\text{-max}}$ (CDA110) of 1.64 and significant thinning with the minimum material thickness of 0.07 mm/0.6 mm (with a thinning ratio of 88.33 %). Similarly, the $PE_{6\text{-max}}$ (SUS304) was strongly thinned with a minimum material thickness of 0.19 mm/1.25 mm (with a thinning ratio of 84.80 %).

Based on the analysis of simulation data, it is evident that the current combinations of subsequent loading lines during the forming process do not meet the required forming components according to the evaluation criteria. However, the analysis provides a basis for exploring more feasible test options by varying the internal pressure values, axial feed displacement, and combinations of load lines as analyzed.

3. 3. Combined internal pressure line *I*2 and axial load line *A*3/*A*4

After comparing the results and analyzing the data from sections 3.1 and 3.2, the research team has decided to maintain a total axial feed value of 30 mm, using the A3 and *A*4 load lines for axial feed, and using the *I*2 load line for internal pressure with maximum values of 75 and 77 MPa. The research team has also combined the internal pressure and axial feed load lines, resulting in three different simulations: P75I2-Af15A3 with $P_{7\text{-max}} = 75$ MPa, P75I2-Af15A4 with $P_{8\text{-max}} = 75$ MPa, and P77I2-Af15A4 with $P_{9\text{-max}} = 77$ MPa. The results of these simulations 7, 8, and 9, are presented in **Fig. 6** in the order of **Fig. 6, *a*–*c***.

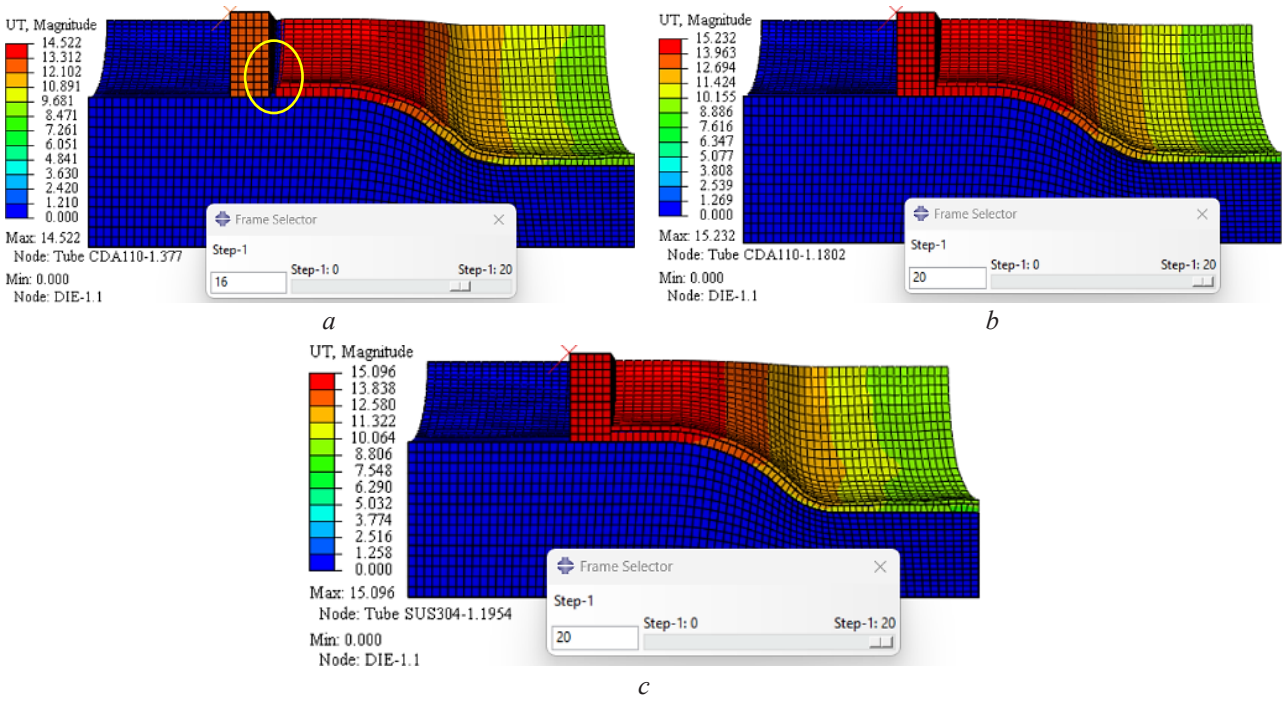

Fig. 6. Shaped bilayer components: *a* – P75I2-Af15A3; *b* – P75I2-Af15A4; *c* – P77I2-Af15A4

Simulation 7 produces satisfactory component profiles with complete expansion of the mold cavity, except for small wrinkled waves in the transition zone of radius *R*2. However, the axial feed is delayed in steps 16 and 17, and the sealing requirement is not met by step 20. The internal pressure $P_{7\text{-max}} = 75$ MPa satisfies the forming pressure condition. Both layers experience plastic deformation with good plastic deformation composition $PE_{7\text{-max}}$ (CDA110) = 1.12, and the thinnest material thickness is 0.36 mm/0.6 mm with a thinning ratio of 40.00 %. $PE_{7\text{-max}}$ (SUS304) = 1.04 and the thinnest material thickness is 0.79 mm/1.25 mm with a thinning ratio of 36.80 %.

Simulation 8 shows that the combination of loading lines is appropriate and guarantees axial feeding while meeting the sealing requirement in 20 steps, ensuring feeding into the extended area. Both layers of materials are plastically deformed and shaped well with $PE_{8\text{-max}}$ (CDA110) of 0.78 and thinned in guiding and extension zones with a minimum thickness of 0.37 mm/0.6 mm (thinning ratio of 38.33 %); and $PE_{8\text{-max}}$ (SUS304) of 0.68 and thinned in guiding and expansion zones with a minimum thickness of 0.86 mm/1.25 mm (thinning ratio of 31.20 %). The component profile is well-formed, except for a small area in the transition zone of radius R_2, where the expanded material is not close to the cavity contour.

Simulation 9 produced satisfactory results with a suiTable combination of loading lines resulting in guaranteed axial feed into the extended zone and sealing requirements in all 20 steps of the process. Both layers of material were plastically deformed, with plastic deformation component $PE_{\max}$ (CDA110) at 1.003 and thinned in the guiding and expansion zones, with the thinnest material thickness at 0.40 mm/0.6 mm and a thinning ratio of 33.33 %; $PE_{\max}$ (SUS304)

was at 0.918, and thinned in the conduction and extension regions, with the thinnest material thickness at 0.85 mm/1.25 mm and a thinning ratio of 32 % (**Fig. 8, *e–h***). The component profile was well-formed, and the transition zone with radii R_1 and R_2 had the material expanded according to the cavity profile.

The research team has evaluated the output criteria of the forming process and identified an optimal combination of loading lines that results in good formability (**Fig. 7**). With this information, the team has determined the optimal combination plan for the 2-layer tube hydrostatic forming process. The simulation results of this plan are displayed in **Fig. 8**.

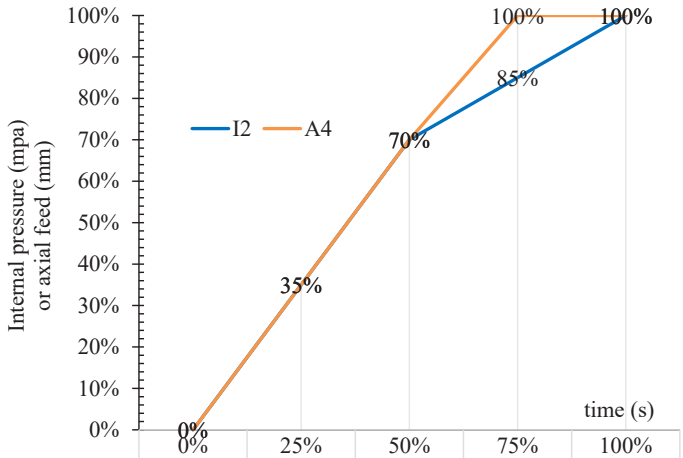

	0%	25%	50%	75%	100%
I2	0	0.35	0.7	0.85	1
A4	0	0.35	0.7	1	1

Fig. 7. Optimum combination of internal pressure load line I2 and axial feed load line *A*4

It is worth noting that the Von Mises stress values of 423.45 MPa for layer CDA110 and 578.96 MPa for layer SUS304, represent the maximum stress values reached during the forming process. These values are equivalent to the ultimate tensile strength of the respective layers, which means that the material is under very high stress and may be close to or at the point of failure. Therefore, it is important to ensure that the maximum stress values do not exceed the ultimate tensile strength of the materials in order to avoid material failure and maintain the integrity of the formed component.

The total reaction force *RF* (**Fig. 8, *d***) can be broken down into three individual forces, which include F_z, F_p, and F_f. The axial force component F_z initiates in the tube wall and, in conjunction with the internal pressure, ensures the plastic flow of the tube wall. The sealing force F_p results from the reaction force of the internal pressure on the front punch face. Finally, the frictional force F_f must be overcome in the section where the tube ends come into contact with the hydroforming tool during the forming process. The maximum absolute value of the total reaction force *RF* exerted by the axial punch is 14270 N, which is equivalent to 1,470 tons.

Through numerical simulation, the group has a scientific basis to solve the problem under study, which is reflected in features such as combining different load lines with different internal pressure values of $P_{i\text{-max}}$, different axial feeding values of *Af* to evaluate the ability to form a two-layer stepped hollow shaft with maximum expanded diameter $D_e = 1.8D0 = 1.8\times21.80 = 39.24$ (mm) through four output criteria. Based on that, the optimal combination of load lines and $P_{i\text{-max}} = 77$ MPa, $Af_{\text{total-max}} = 30$ mm values was found to increase the likelihood of successful formation in the hydroforming process of two different layers of tubing, with the outer layer being SUS304 stainless steel and the inner layer being CDA110 copper material (**Fig. 7**). The uniqueness and novelty of the results are specifically confirmed through the Plastic strain component of layer SUS304 at 0.918 and the Plastic strain component of layer CDA110 at 1.003, as well as the wall thinning ratio at 32 % and 33.33 % (the allowable limit is 45 %) which are quite similar in order (**Fig. 8, *e–h***).

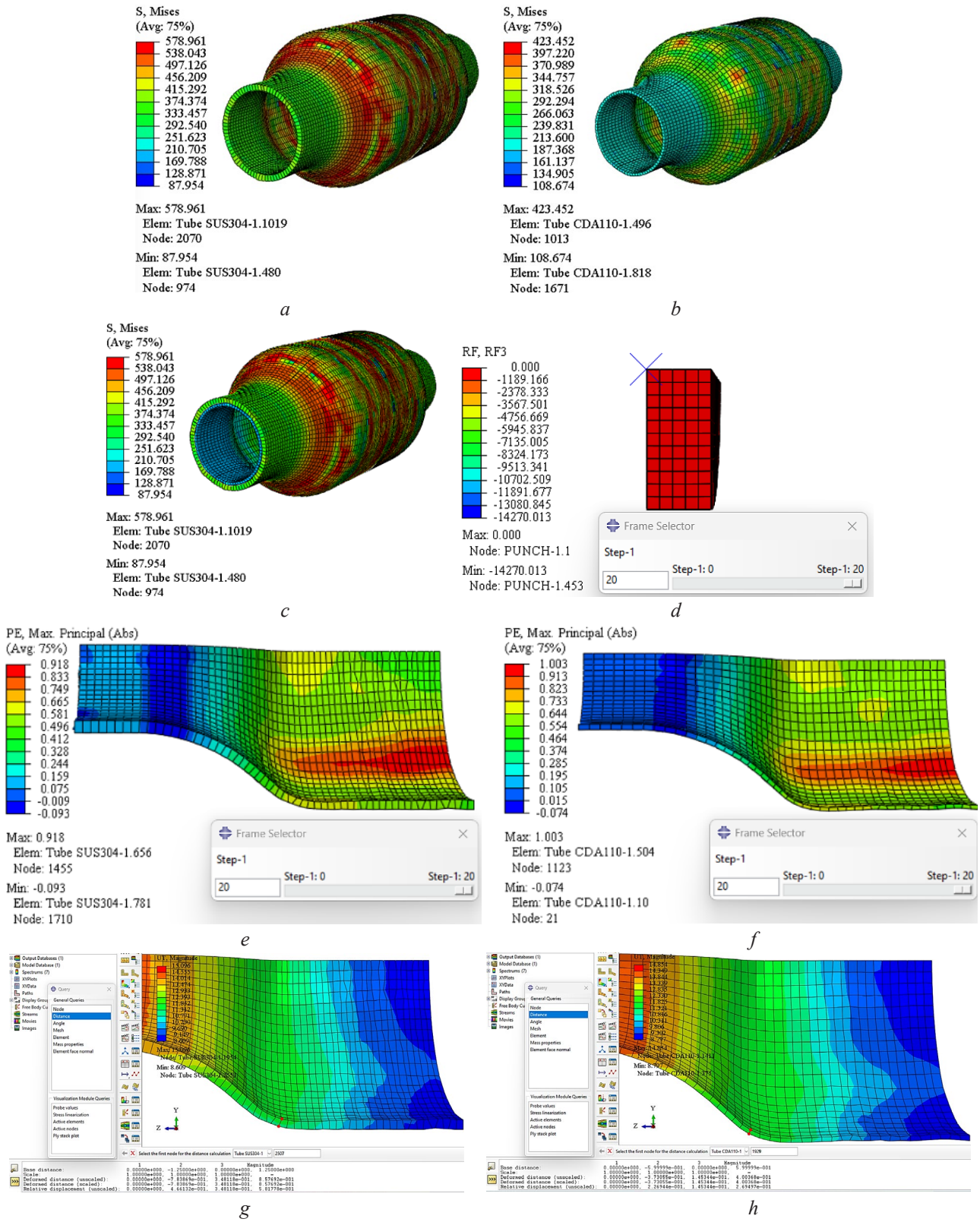

Fig. 8. Output parameters of the two-layer component formed with the optimal combination of P77I2 – Af15A4 lo ad lines: *a* – Von Mises stress of layer SUS304; *b* – Von Mises stress of layer CDA110; *c* – Von Mises stress of 2-layer component; *d* – Total reaction force of axial punch; *e* – Plastic strain component of layer SUS304; *f* – Plastic strain component of layer CDA110; *g* – Minimum thickness measurement of layer CDA110; *h* – Minimum thickness measurement of layer SUS304

Fig. 7 shows that the axial feeding load line *A*4 increases the feeding more than the internal pressure load line *I*2 at the time when the time of the forming process reaches 50 %, to ensure feeding into the expanded region in time. The axial feeding of each axial punch reaches the value of Af_{max} = 15 mm at the time of 75 % of the forming process time, and in the time interval from 75 % to 100 % of the forming process time, the axial punch acts to seal both ends of the tube while the fluid pressure continues to advance towards $P_{i\text{-max}}$ = 77 MPa along load line *I*2. The time cycle of the forming process based on numerical simulation is divided into 20 forming steps, which is quite consistent with the statistics on the time cycle of the actual forming process [13, 26].

The limitations of the research results of the research group include the boundary conditions of friction being set only at a common friction coefficient value of $\mu = 0.1$, and the time cycle of the forming process being set according to the number of forming simulation steps (20 forming steps).

To increase the applicability of the obtained results in reality, it is necessary to control issues such as lubrication of the surface of the tube blank and the mold surface to ensure stable friction coefficient in all 3 zones (the guiding zone, the transition zone, and the expansion zone), as well as the synchronized combination of the internal pressure loading line *I*2 and the axial feed loading line *A*4 from the execution devices according to the forming steps. They are truly an interesting challenge and attract further development research in some directions such as expanding the value range of the friction coefficient, expanding the value range of the thickness of each layer, expanding the range of loading paths, and finding the relationship between the real-time cycle and the number of forming steps in the numerical simulation for the forming process of 2-layer tube blanks made of different materials.

Running simulations with other combined options can provide researchers with more data to better understand how different shaping parameters impact the hydrostatic forming process of multilayer tubes. This can help identify additional optimal combinations of load lines and lubrication conditions, as well as provide insights into the effects of variations in these parameters on the output criteria of the forming process.

4. Conclusions

Numerical simulation offers the ability to combine various loading paths to optimize the output criteria when forming a 2-layer metal pipe product using hydrostatic forming. This technique has been extensively documented in publications, highlighting its advantages. However, in practical applications such as experimental deployment and production, controlling the load paths and their combination, as well as lubrication, pose challenges in implementing the 2-layer product hydrostatic forming process.

Through a comparison of simulation results of different load line combinations, the research team was able to determine the optimal combination of pressure load line *I*2 ($P_{i\text{-max}}$ = 77 MPa) and axial feed line A4 (with total axial feed displacement of 2 punches of 30 mm), based on four criteria including Von Mises stress, plastic strain component (PE), wall thinning, and pipe profile. Of note, this optimal combination resulted in the SUS304 and CDA110 layers having a similar PE plastic strain component of approximately 1, and a similar wall thinning ratio, without any material delamination occurring.

Conflict of interest

The authors declare that they have no conflict of interest in relation to this research, whether financial, personal, authorship or otherwise, that could affect the research and its results presented in this paper.

Financing

The first author acknowledges financial support from the Scholarship Council of University of Economics and Technology (UNETI) (No. 99/QĐ-ĐHKTKTCN) for his research at HaNoi University of Science and Technology in Vietnam.

Data availability

Data will be made available on reasonable request.

Acknowledgments

The team of authors would like to express their gratitude for the help of the University of Economics and Technology for Industries (https://uneti.edu.vn/) and HaNoi University of Science and Technology (https://www.hust.edu.vn/) during the implementation of this study.

References

[1] Bell, C., Corney, J., Zuelli, N., Savings, D. (2019). A state of the art review of hydroforming technology. International Journal of Material Forming, 13 (5), 789–828. doi: https://doi.org/10.1007/s12289-019-01507-1

[2] Fiorentino, A., Ginestra, P. S., Attanasio, A., Ceretti, E. (2020). Numerical Optimization of the Blank Dimensions in Tube Hydroforming Using Line-Search and Bisection Methods. Materials, 13 (4), 945. doi: https://doi.org/10.3390/ma13040945

[3] Kocańda, A., Sadłowska, H. (2008). Automotive component development by means of hydroforming. Archives of Civil and Mechanical Engineering, 8 (3), 55–72. doi: https://doi.org/10.1016/s1644-9665(12)60163-0

[4] Han, S., Woo, Y., Hwang, T., Oh, I., Moon, Y. H. (2019). Tailor layered tube hydroforming for fabricating tubular parts with dissimilar thickness. International Journal of Machine Tools and Manufacture, 138, 51–65. doi: https://doi.org/10.1016/j.ijmachtools.2018.11.005

[5] Saboori, M., Gholipour, J., Champliaud, H., Wanjara, P., Gakwaya, A., Savoie, J. (2016). Prediction of Burst Pressure in Multistage Tube Hydroforming of Aerospace Alloys. Journal of Engineering for Gas Turbines and Power, 138 (8). doi: https://doi.org/10.1115/1.4032437

[6] Sadłowska, H., Kochański, A., Czapla, M. (2020). Application of the Numerical Model to Design the Geometry of a Unit Tool in the Innovative RTH Hydroforming Technology. Materials, 13 (23), 5427. doi: https://doi.org/10.3390/ma13235427

[7] Fassi, I., Shipley, D. (Eds.) (2017). Micro-Manufacturing Technologies and Their Applications. Springer, 296. doi: https://doi.org/10.1007/978-3-319-39651-4

[8] Ngaile, G., Lowrie, J. (2014). New Micro Tube Hydroforming System Based on Floating Die Assembly Concept. Journal of Micro and Nano-Manufacturing, 2 (4). doi: https://doi.org/10.1115/1.4028320

[9] Hartl, C., Schiefer, H., Chlynin, A. (2014). Evaluation of experimental and numerical investigations into micro-hydroforming of platinum tubes for an industrial application. Manufacturing Review, 1, 17. doi: https://doi.org/10.1051/mfreview/2014015

[10] Duc Quang, V., Van Duy, D., Dac Trung, N. (2021). On the Formation of Protrusion and Parameters in the Tube Hydroforming. Mechanisms and Machine Science, 521–530. doi: https://doi.org/10.1007/978-3-030-91892-7_49

[11] Duc, Q. V., Van, D. D., Dac, T. N., Huu, Q. N. (2022). Quality comparison of Y-shape joints by tube hydroforming with and without counterforce. EUREKA: Physics and Engineering, 4, 46–56. doi: https://doi.org/10.21303/2461-4262.2022.002256

[12] Abbassi, F., Ahmad, F., Gulzar, S., Belhadj, T., Karrech, A., Choi, H. S. (2020). Design of T-shaped tube hydroforming using finite element and artificial neural network modeling. Journal of Mechanical Science and Technology, 34 (3), 1129–1138. doi: https://doi.org/10.1007/s12206-020-0214-4

[13] Singh, H. (2003). Fundamentals of hydroforming. The Society of Manufacturing Engineers.

[14] Cherouat, A., Saanouni, K., Hammi, Y. (2002). Numerical improvement of thin tubes hydroforming with respect to ductile damage. International Journal of Mechanical Sciences, 44 (12), 2427–2446. doi: https://doi.org/10.1016/s0020-7403(02)00177-7

[15] Wei, W., Zhang, W., Wei, K. X., Zhong, Y., Cheng, G., Hu, J. (2009). Finite element analysis of deformation behavior in continuous ECAP process. Materials Science and Engineering: A, 516 (1-2), 111–118. doi: https://doi.org/10.1016/j.msea.2009.03.001

[16] Pandey, A. K., Walunj, B. S., Date, P. P. (2018). Simulation based approach for light weighting of transmission components using tube hydroforming. Procedia Manufacturing, 15, 915–922. doi: https://doi.org/10.1016/j.promfg.2018.07.405

[17] Chung, K., Alexandrov, S. (2007). Ideal Flow in Plasticity. Applied Mechanics Reviews, 60 (6), 316–335. doi: https://doi.org/10.1115/1.2804331

[18] Chung, K., Richmond, O. (1992). Ideal forming—II. Sheet forming with optimum deformation. International Journal of Mechanical Sciences, 34 (8), 617–633. doi: https://doi.org/10.1016/0020-7403(92)90059-p

[19] Alexandrov, S., Lyamina, E., Lang, L. (2021). Description of the Expansion of a Two-Layer Tube: An Analytic Plane-Strain Solution for Arbitrary Pressure-Independent Yield Criterion and Hardening Law. Metals, 11 (5), 793. doi: https://doi.org/10.3390/met11050793

[20] Mori, S., Manabe, K.-I., Nishimura, H. (1990). Hydraulic bulge forming of clad thin-walled tubes. Adv. Tech. Plast, 3, 1549–1554.

[21] Mac Donald, B. J., Hashmi, M. S. J. (2000). Finite element simulation of bulge forming of a cross-joint from a tubular blank. Journal of Materials Processing Technology, 103 (3), 333–342. doi: https://doi.org/10.1016/s0924-0136(00)00522-7

[22] Olabi, A. G., Alaswad, A. (2011). Experimental and finite element investigation of formability and failures in bi-layered tube hydroforming. Advances in Engineering Software, 42 (10), 815–820. doi: https://doi.org/10.1016/j.advengsoft.2011.05.022

[23] Hossein Seyedkashi, S. M., Panahizadeh R, V., Xu, H., Kim, S., Moon, Y. H. (2013). Process analysis of two-layered tube hydroforming with analytical and experimental verification. Journal of Mechanical Science and Technology, 27 (1), 169–175. doi: https://doi.org/10.1007/s12206-012-1216-7

[24] Payganeh, M. Gh., Chaeichi siahkal, O., Malekzadeh Fard, K., Shahbazi Karami, J. (2017). Experimental Study and Simulation of Tube Hydroforming Process of Bi-layered Aluminum-Copper with Axial Feeding. Journal of Applied and Computational Sciences in Mechanics, 28 (2), 65–84. doi: https://doi.org/10.22067/FUM-MECH.V28I2.48455

[25] Abaqus/Explicit 3D EXPERIENCE R2017X.

[26] Koç, M. (Ed.) (2008). Hydroforming for advanced manufacturing. Woodhead Publishing. doi: https://doi.org/10.1533/9781845694418

Received date 28.02.2023
Accepted date 07.05.2023
Published date 27.07.2023

© The Author(s) 2023
This is an open access article
under the Creative Commons CC BY license

How to cite: *Vu, Q. D., Nguyen, T. D., Dang, H. V., Phan, D. T. (2023). Effect of loading paths on hydroforming ability of stepped hollow shaft components from double layer pipes. EUREKA: Physics and Engineering, 4, 143–154. doi: https://doi.org/10.21303/2461-4262.2023.002797*